

MHD instabilities in astrophysical plasmas: very different from MHD instabilities in tokamaks!

J. P. Goedbloed

*FOM Institute DIFFER – Dutch Institute for Fundamental Energy Research –
Eindhoven, the Netherlands*

Abstract

The extensive studies of MHD instabilities in thermonuclear magnetic confinement experiments, in particular of the tokamak as the most promising candidate for a future energy producing machine, have led to an ‘intuitive’ description based on the energy principle that is very misleading for most astrophysical plasmas. The ‘intuitive’ picture almost directly singles out the dominant stabilizing field line bending energy of the Alfvén waves and, consequently, concentrates on expansion schemes that minimize that contribution. This happens when the wave vector \mathbf{k}_0 of the perturbations, on average, is perpendicular to the magnetic field \mathbf{B} . Hence, all macroscopic instabilities of tokamaks (kinks, interchanges, ballooning modes, ELMs, neoclassical tearing modes, etc.) are characterized by satisfying the condition $\mathbf{k}_0 \perp \mathbf{B}$, or nearly so. In contrast, some of the major macroscopic instabilities of astrophysical plasmas (the Parker instability and the magneto-rotational instability) occur when precisely the opposite condition is satisfied: $\mathbf{k}_0 \parallel \mathbf{B}$. How do those instabilities escape from the dominance of the stabilizing Alfvén wave? The answer to that question involves, foremost, the recognition that MHD spectral theory of waves and instabilities of laboratory plasmas could be developed to such great depth since those plasmas are assumed to be in *static* equilibrium. This assumption is invalid for astrophysical plasmas where rotational and gravitational accelerations produce equilibria that are at best *stationary*, and the associated spectral theory is widely, and incorrectly, believed to be non-self adjoint. These complications are addressed, and cured, in the theory of *the Spectral Web*, recently developed by the author. Using this method, an extensive survey of instabilities of astrophysical plasmas demonstrates how the Alfvén wave is pushed into insignificance under these conditions to give rise to a host of instabilities that do not occur in laboratory plasmas.

1. Misleading ‘intuition’

Magnetohydrodynamic (MHD) instabilities have been a constant worry in magnetic fusion research. Theory has focused on the analysis of the multifarious MHD modes, frequently exploiting large-scale numerics, whereas experiment has been successful in ever expanding the duration of stable confinement from the microseconds in the 1960s to the present time scale of minutes. Major disruptions remain a source of concern, but various scenarios have been devised to control their effects. At any rate, the extensive body of results on MHD modes has been impressive enough to become exemplary for a reliable scientific enterprise. Presentations of this activity are often preceded by a so-called ‘intuitive picture’ of the MHD instabilities by means of the energy principle [1], where trial functions are substituted in the energy functional $W[\xi]$ to find out whether $W > 0$ for all ξ (stable) or not (unstable). This approach provides basic insight in the dynamics of simple kink modes as well as the intricate dynamics of ballooning modes in complex magnetic geometries. Except for the obvious limitations of the MHD model,

generally recognized and addressed by the development and operation of hybrid MHD-particle codes, two less obvious limitations are usually not taken as seriously as they should:

(a) The equilibrium itself becomes very different from a tokamak equilibrium if gravity and rotation come into play, as is the case for all astrophysical plasmas. Tokamaks have a dominant magnetic field that is approximately force-free, so that the equilibria may be considered as low- β , *magneto*-hydrodynamic:

$$\mathbf{j} \times \mathbf{B} = \nabla p \sim \beta \ll 1. \quad (1)$$

Many astrophysical plasmas have dominant gravitational accelerations ($\mathbf{g} = -\nabla\Phi$) and rotations that are approximately Keplerian, whereas the magnetic field is frequently a small (but crucial) correction, so that the equilibria should be considered as high- β , *hydro*-magnetic:

$$\rho \mathbf{v} \cdot \nabla \mathbf{v} + \rho \nabla \Phi + \nabla p = \mathbf{j} \times \mathbf{B} \sim \beta^{-1} \ll 1. \quad (2)$$

(b) For static equilibria described by Eq. (1), expansion of the energy principle in powers of the inverse aspect ratio nearly directly leads to the dominance of the Alfvén mode contribution,

$$W \approx \frac{1}{2} \int (\mathbf{k}_0 \cdot \mathbf{B})^2 |\xi_n|^2 dV \gg 0. \quad (3)$$

(See, e. g., the first term of Eq. 17.40 in the derivation of the spectral variational principle for static toroidal plasmas in Ref. [2], p. 318.) Hence, instabilities must have wave vectors \mathbf{k}_0 perpendicular, or nearly perpendicular, to the magnetic field \mathbf{B} in order for the higher order curvature effects, of e.g. ballooning modes, to have a chance to contribute. This line of reasoning, and the extensive body of intuition based on it, is not valid for instabilities operating in stationary equilibria described by Eq. (2). It is even in evident conflict with one of the basic astrophysical instabilities, where rotation does not play a role, viz. the Parker instability, operating in static equilibria where Eq. (1) is just extended with the gravitational term $\rho \nabla \Phi$. That instability requires the wave vector to be parallel, or nearly parallel, to the magnetic field and thus appears to escape the dominance of the Alfvén modes.

We will analyze how these facts completely change the theory of astrophysical instabilities compared to their laboratory counterparts, and illustrate this with the Parker, the Rayleigh–Taylor, and the magneto-rotational instability (MRI).

2. The Parker instability (gravity)

The Parker instability [3] has been introduced to explain the tendency of the interstellar plasma in spiral arms to form clouds. It was thought to be “related to the magnetic Rayleigh–Taylor instability”. That instability is, in turn, related to the interchange instability operating in magnetically confined plasmas in magnetic fusion devices, where the gravitational driving term of the density gradient, $\rho'g$, is replaced by the negative pressure gradient, p' . Thus, the gravitational interchange instability criterion, violation of $\rho'g + \rho^2 g^2 / (\gamma p) \leq \frac{1}{4} B^2 \phi'^2$, where ϕ' is the magnetic shear, turns out to be completely analogous to Suydam’s criterion in cylindrical geometry (or Mercier’s criterion in toroidal geometry) for local instabilities in tokamaks. The analogous analysis is based on the mentioned assumption $\mathbf{k}_0 \cdot \mathbf{B} \approx 0$ to kill the enormous stabilizing field line bending energy (3) of the Alfvén waves.

Now consider Fig. 1 (from Ref. [2]), which shows the complete spectrum of a gravitating magnetized plasma slab ($0 \leq x \leq 1$) of thickness a , exponential density and pressure, $\rho = \rho_0 e^{-\alpha x}$ and $p = p_0 e^{-\alpha x}$, and sheared magnetic field $\mathbf{B} = B_0 e^{-\frac{1}{2}\alpha x} [\sin(\lambda x)\mathbf{e}_y + \cos(\lambda x)\mathbf{e}_z]$. [The parameters are: $\alpha \equiv \rho_0 g / (p_0 + \frac{1}{2}B_0^2)$, $\beta \equiv 2p_0 / B_0^2$, λ , fixed at $\alpha = 20$, $\beta = 0.5$, $\lambda = 0.3$, and $k_0^2 \equiv k_y^2 + k_z^2 = 10$.] The squared wave frequency $\bar{\omega}^2$, or instability growth rate (if $\bar{\omega}^2 < 0$), is plotted versus the direction ϑ of the wave vector \mathbf{k}_0 . For $\vartheta \approx \frac{1}{2}\pi$ (or $\mathbf{k}_0 \cdot \mathbf{B} \approx 0$), the familiar degeneracy of Alfvén and slow mode frequencies is obtained, together with the clustering of infinitely many interchange modes. Their growth rates are dwarfed though compared to those of the Parker instabilities that occur for $\vartheta \approx 0$ (where \mathbf{k}_0 is approximately parallel \mathbf{B}). This, at once, resolves the apparent contradiction with standard tokamak stability theory: The Parker instabilities are part of the slow mageto-acoustic sub-spectrum, with eigenfunction polarizations orthogonal to those of the Alfvén waves. This is the way these astrophysical instabilities escape the Alfvén wave dominance that reigns in the tokamak regime.

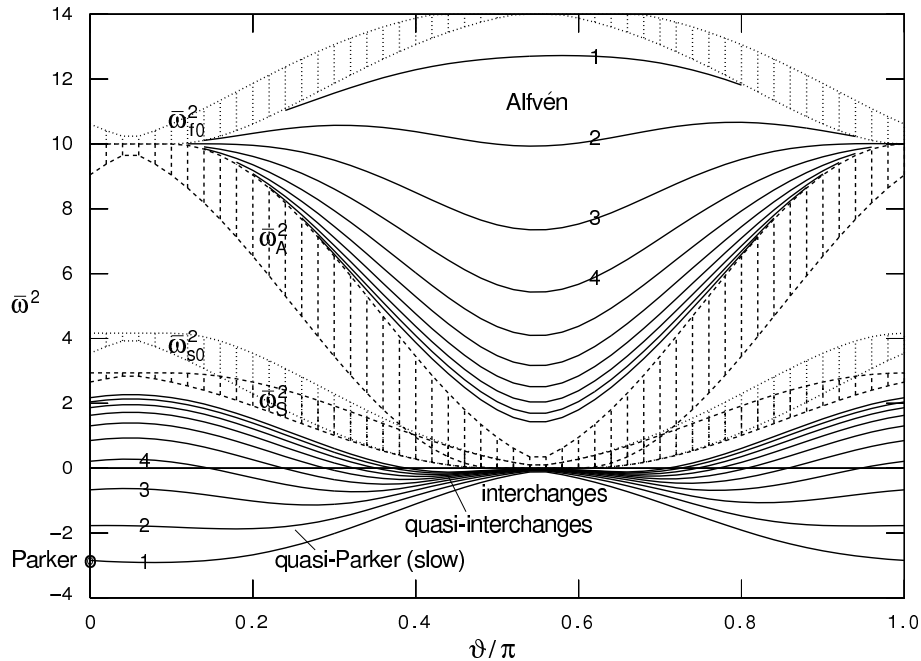


Figure 1: *Spectrum of Alfvén and slow magneto-acoustic modes of a gravitating plasma as a function of the angle ϑ between horizontal wave vector and magnetic field. The Parker and quasi-Parker instabilities connect smoothly to the interchange and quasi-interchange instabilities (related to similar modes in tokamaks). Modes with vertical mode numbers $n = 1, 2, \dots$ approach the continua $\{\omega_A^2\}$ and $\{\omega_S^2\}$.*

3. The Spectral Web

The systematic theory of the spectrum of MHD waves and instabilities of magnetized plasmas has mainly been developed for static equilibria, where the energy principle has been the standard stability paradigm for over half a century. However, most plasmas in magnetic fusion devices have substantial flows, and in astrophysics the paradigm simply makes no sense because there are no static plasmas in the Universe. The required modification for stationary equilibria has been known since the appearance of the seminal paper by Frieman and Rotenberg [4] in 1960, but, unfortunately, further development of spectral theory along this line has been hampered by

the general misunderstanding that this theory necessarily involves non-self-adjoint operators. A new approach, exploiting what will be called the *Spectral Web*, is based on the opposite observation, viz. that the Frieman–Rotenberg spectral equation,

$$\mathbf{G}(\xi) - 2\rho\omega U\xi + \rho\omega^2\xi = 0, \quad (4)$$

is a non-linear eigenvalue problem involving *two self-adjoint operators*, viz. the generalized force operator \mathbf{G} and the Doppler–Coriolis operator $U \equiv -iv_0 \cdot \nabla$. With these operators two real quadratic forms may be associated, viz. the solution averages of the potential energy W and of the Doppler–Coriolis shift V of the perturbations. For complex $\omega = \sigma + iv$, where the imaginary part v corresponds to the growth rates of instabilities, the real part corresponds to the solution averages of the Doppler–Coriolis shift: $\sigma \equiv \text{Re}(\omega) = \bar{V}$.

The usual proof of self-adjointness of the force operator is modified by exploiting, for arbitrary values of ω , the left solution ξ^ℓ of Eq. (4) that satisfies the BCs on axis and the right solution ξ^r that satisfies the BCs at the wall. The two solutions are joined at some surface S inside the plasma. At that surface, the surface energy W_{com} is constructed,

$$W_{\text{com}} = -\frac{1}{2} \int \xi_n^* [[\Pi(\xi)]] dS, \quad (5)$$

where the normal component ξ_n is made continuous and the jump $[[\Pi(\xi)]]$ of the total pressure perturbation does not vanish, in general. This *complementary energy* represents the amount of energy to be injected or extracted at S to obtain exponential time behavior $\exp(-i\omega t)$. Self-adjointness implies that W_{com} vanishes, which is the case for eigenvalues. Instead, in the method of the Spectral Web, the real and imaginary parts of W_{com} are contour plotted to obtain two sets of curves in the complex ω -plane on which one of the two vanishes:

$$\text{Im}[W_{\text{com}}(\omega)] = 0 \Rightarrow \textit{solution path}, \quad \text{Re}[W_{\text{com}}(\omega)] = 0 \Rightarrow \textit{conjugate path}. \quad (6)$$

The eigenvalues are located at the intersections of these two curves. Thus, for the first time, the general eigenvalue problem of stationary equilibria is solved by an intuitive method that not only provides the complex eigenvalues of the instabilities, but also connects them with physically meaningful curves. The method is applied to the instabilities of a straight cylinder, for which the reduction of the Frieman–Rotenberg equation (4) is well documented [5, 6]. The Spectral Web method is not restricted to cylindrical problems though since reduction to ordinary differential equations in the normal direction for ξ_n and Π also obtains for toroidal problems where the tangential dependences are taken care of by a separate reduction. The earlier papers on the subject of constructing the eigenvalues of stationary equilibria [7] are now superseded by the present form of the method of the Spectral Web [8].

Note that the functions ξ exploited in the Solution Web method are not smooth trial functions, as in the energy principle, but full solutions of the actual physical problem posed by the Frieman–Rotenberg equation (4). Those solutions are not yet eigenfunctions though since they exhibit a jump at the surface S . The method relies on the fact that the numerical solution of ordinary or partial differential equations is presently straight-forward, but this does not apply to the solution of eigenvalue problems. That part is addressed by the construction of the two sets of curves in the complex ω -plane by means of contour plotting. Their construction is straight-forward as well and, moreover, it can be implemented numerically in a trivially parallel manner

since all computations for the different values of ω can be done simultaneously. The solution path and the conjugate path may be considered as the loci of points in the complex ω -plane where the physical problem of a driven system is solved: excitation in-phase for the solution path and excitation out-of-phase for the conjugate path. Where the two curves intersect, the actual eigenvalue problem is solved since driving does not require any energy then: the jump vanishes and $W_{\text{com}} = 0$.

4. The Rayleigh–Taylor instability (rotation)

Fig. 2 shows the Spectral Web, consisting of the solution path (in red) and the conjugate path (in blue), with the eigenvalues (black dots) at the intersections, for the Rayleigh–Taylor instabilities of a rotating plasma cylinder with a longitudinal magnetic field B_z (a rotating θ -pinch). The equilibrium is fixed by choosing a constant angular velocity $\Omega \equiv v_\theta/r$ and the following profiles: $\rho(r) = \rho_0 \cosh^{-2} f(x)$, $p(r) = p_0 \cosh^{-2} f(x)$, $B_z(r) = B_\infty (\delta + (1 - \delta) \tanh f(x))$, where $f(x) \equiv \alpha^2 (x^2 - x_0^2)$ with $x \equiv r/a$. [The parameters for this case are: $x_0 = 0$, $\alpha = 2$, $\delta = 0.1667$.] The Spectral Web shown is for the compressible $m = 1$, $k = 0$ modes, so that $\mathbf{k}_0 \cdot \mathbf{B} = kB_z = 0$ for these modes, but the point is that the magnetic field does not enter at all here: These are purely hydrodynamic modes with a clustering point at the hydrodynamic flow continuum $\Omega_0 = mv_\theta/r$. This continuum is degenerate (indicated by the big red dot in the main frame of Fig 2).

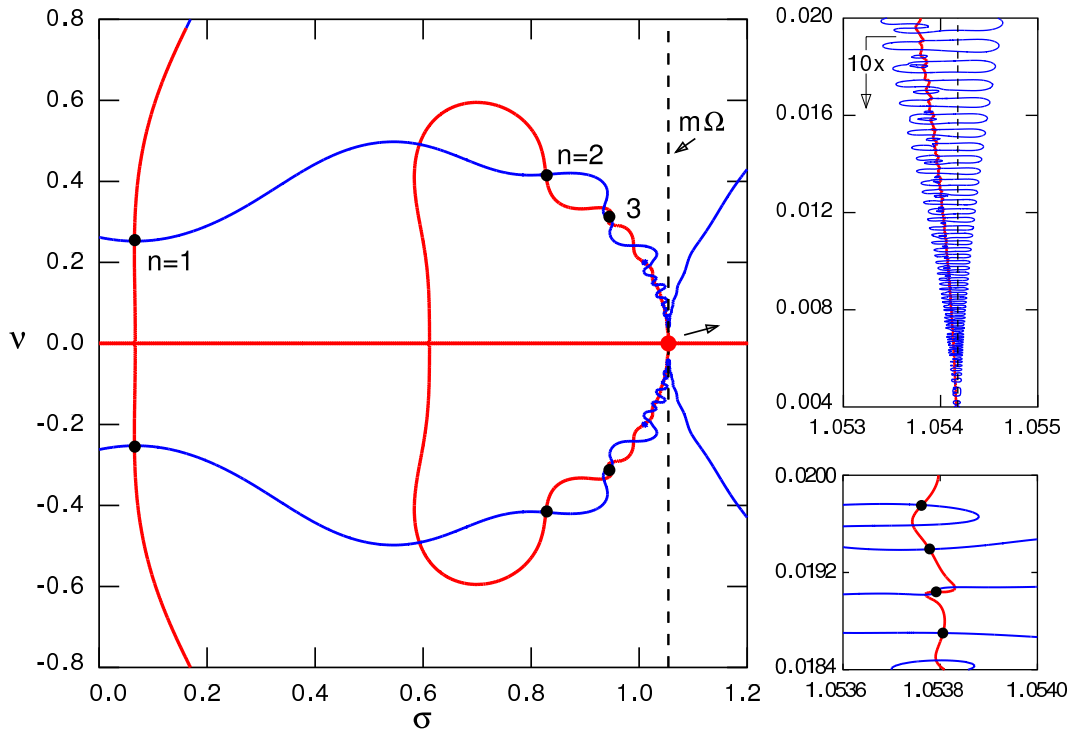


Figure 2: Spectral Web for the $m = 1$, $k = 0$ hydrodynamic Rayleigh–Taylor instabilities of a rotating plasma cylinder. The side frame shows the cluster sequence toward the flow continuum (red dot in the main frame), with a zoom of the $n = 53, \dots 56$ eigenvalues in the bottom frame.

The most striking feature of the Spectral Web of the hydrodynamic Rayleigh–Taylor instabilities is the fact that the solution path is not a single curve, as one might have expected, but it is split into a separate open curve with the most global $n = 1$ mode on it and a closed loop with

the $n = 2$ mode and all the rest of infinitely many clustering modes. The latter have a Doppler shifted frequency $\tilde{\sigma} \equiv \sigma - m\Omega$ which tends to zero, whereas the most global modes have a large Coriolis shift, opposite to the Doppler shift, such that the combined Doppler–Coriolis shift, and hence σ , may become small. Another striking feature is that the $n = 2$ mode has a larger growth rate than the $n = 1$ mode. Such behavior never occurs for static equilibria.

Hence, the Spectral Web method addresses the problem of constructing the complex eigenvalues of a stationary equilibrium (usually, and erroneously, assumed to be intrinsically non-selfadjoint) by contour plotting the complementary energy W_{com} in the complex ω -plane. This generates two sets of curves in the ω -plane, *the solution path*, where W_{com} is real, and *the conjugate path*, where W_{com} is imaginary. The eigenvalues are found at the intersections of those paths: $W_{\text{com}} = 0$. The crucial difference with the spectral theory of static plasmas, relevant for tokamaks, is the occurrence of two operators, viz. the generalized force operator \mathbf{G} and the gradient operator $U \equiv -i\mathbf{v} \cdot \nabla$, which are both self-adjoint. The later operator generates the Doppler–Coriolis shift of the eigenvalues away from the imaginary axis (where they reside for static equilibria): a big effect in Fig. 2 for the $m = 1$ modes.

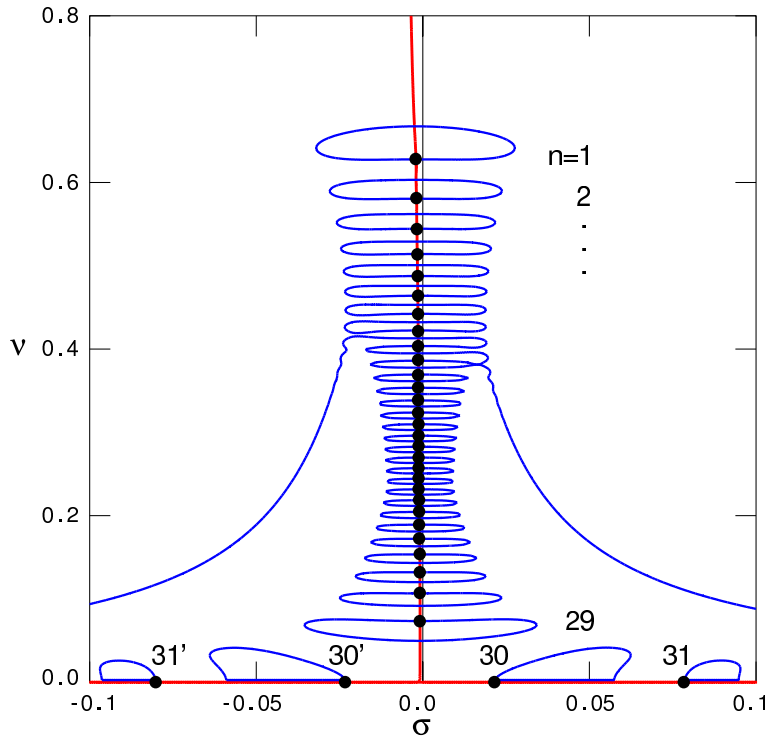


Figure 3: *Spectral Web of the magneto-rotational instabilities (MRIs) for a thin accretion disk with mode numbers $m = 0$, $k = 70$. The solution path is red, conjugate path is blue, eigenvalues at the intersections are indicated by black dots ($n = 1-29$ for the instabilities and $n = 30, 30', 31, 31'$ for the stable modes).*

5. The Magneto-Rotational instability (gravity and rotation)

Fig. 3 illustrates yet another class of astrophysical instabilities that require completely different analysis than the one used for tokamaks. It shows the discrete spectrum of magneto-rotational instabilities (MRIs) [9] of a thin annular ($r_1 \leq r \leq r_2$) accretion disk for a self-similar equilibrium [10] $\rho \sim r^{-3/2}$, $v_\theta \sim r^{-1/2}$, $\sqrt{p} \sim B_z \sim B_\theta \sim r^{-5/4}$. [The physical variables are

normalized by setting $r_1 = \rho_1 = GM_* = 1$ at the inner radius, the parameters are then given by $\delta \equiv r_2/r_1$, $\varepsilon \equiv \sqrt{p_1}$, $\beta \equiv 2p_1/B_1^2$, $\mu \equiv B_{\theta 1}/B_{z 1}$, for this case fixed at $\delta = 2.0$, $\varepsilon = 0.1$, $\beta = 100$, $\mu = 1$.] The nonlinear turbulent phase of the MRIs is assumed to provide the source of anomalous dissipation needed to account for the loss of angular momentum of accretion disks about black holes and other compact objects [11].

The equations for the MHD spectrum of the MRIs of a thin cylindrical accretion disk were derived by Keppens *et al.* [12]. The spectrum shown in Fig. 3 was computed by the new method of the Spectral Web. It shows the solution path (the red curve slightly deviating from the imaginary axis) and the conjugate paths (the blue ‘pancakes’) for the axi-symmetric modes ($m = 0$). This implies that the Doppler shift vanishes, $\tilde{\omega} \equiv \omega$, but the small Coriolis shift moves the eigenvalues off the imaginary axis. Because $m = 0$ in this case, the combined Doppler–Coriolis shift of the eigenvalues off the imaginary axis is a small effect. For non-axisymmetric modes, the solution path is far away though from the imaginary axis.

Clearly, the magneto-rotational instabilities violate ‘the tokamak paradigm’ $\mathbf{k}_0 \cdot \mathbf{B} \approx 0$, since they occur far away from the backward and forward Alfvén continua (situated along the real axis outside the frame, at $\sigma \leq -0.5$ and $\sigma \geq 0.5$). where that condition would be satisfied.

6. Conclusions

In conclusion: The global instabilities of both laboratory and astrophysical plasmas can be described by the ideal MHD equations because they are *scale-independent* [13]. However, the major gravitational and rotational effects on astrophysical plasma equilibria completely upset the standard tokamak paradigm for static equilibria, described by Eq. 1, to look for instabilities with $\mathbf{k}_0 \cdot \mathbf{B} \approx 0$ to eliminate the dominant stabilizing Alfvén wave contribution. Instead, a completely different spectral theory is required for the stationary equilibria, described by Eq. 2. The new method of the *Spectral Web* [8] provides an intuitive and efficient tool to construct the complete spectrum of waves and instabilities in the complex plane.

References

- [1] K. Hain, R. Lüst and A. Schlüter, *Z. Naturforsch.* **12a**, 833 (1957);
I. B. Bernstein, E. A. Frieman, M. D. Kruskal and R. M. Kulsrud, *Proc. Roy. Soc. (London)* **A244**, 17 (1958).
- [2] J. P. Goedbloed, R. Keppens and S. Poedts, *Advanced Magnetohydrodynamics* (Cambridge, 2010).
- [3] E. N. Parker, *Astrophys. J.* **145**, 811 (1966); see also review of T. C. Mouschovias, in *Solar and Astrophysical Magnetohydrodynamic Flows*, ed. K. C. Tsinganos (Dordrecht, 1996), pp. 475–504.
- [4] E. Frieman and M. Rotenberg, *Rev. Mod. Phys.* **32**, 898 (1960).
- [5] E. Hameiri, *J. Math. Phys.* **22**, 2080 (1981).
- [6] A. Bondeson, R. Iacono and A. H. Bhattacharjee, *Phys. Fluids* **30**, 2167 (1987).
- [7] J. P. Goedbloed, *Phys. Plasmas* **16**, 122110 & **16**, 122111 (2009).
- [8] J.P. Goedbloed, *43rd EPS Conf. on Plasma Physics*, 4–8 July, Leuven, O3.406 (2016).
- [9] E. P. Velikhov, *Soviet Phys.–JETP Lett.* **36**, 995 (1959);
S. Chandrasekhar, *Proc. Nat. Acad. Sci. USA* **46**, 253 (1960).
- [10] H. C. Spruit, T. Matsuda, M. Inoue and K. Sawada, *Monthly Not. Roy. Astron. Soc.* **229**, 517 (1987).
- [11] S. A. Balbus and J. F. Hawley, *Astron. J.* **376**, 214 (1991).
- [12] R. Keppens, F. Casse and J.P. Goedbloed, *Astrophys. J.* **569**, L121 (2002).
- [13] J. P. Goedbloed and S. Poedts, *Principles of Magnetohydrodynamics* (Cambridge, 2004), p. 138.